Geomorphology 120 (2010) 16–25

Contents lists available at ScienceDirect

Geomorphology

journal homepage: www.elsevier.com/locate/geomorph

Landslide monitoring with high resolution tilt measurements at the Dollendorfer Hardt landslide, Germany

A. García [a,*,1], A. Hördt [b], M. Fabian [c]

[a] Institute of Petroleum Engineering, Reservoir Geophysics Group, Edinburgh Time-lapse Project, Heriot-Watt University, Edinburgh EH14 4AS, UK
[b] Institute of Geophysics and Extraterrestrial Physics, TU Braunschweig, Mendelssohnstr. 3, 38106 Braunschweig, Germany
[c] University of Bremen, Department 5, Geosciences, Sea Technics/Sensors, Klagenfurter Str., D-28359, Bremen, Germany

ARTICLE INFO

Article history:
Received 2 September 2005
Accepted 7 August 2009
Available online 9 October 2009

Keywords:
Landslide
Soil deformation
Tiltmeter
Pore water pressure

ABSTRACT

To continuously monitor ground movement at the Dollendorfer Hardt landslide in Königswinter/Bonn, Germany, a borehole and a platform tiltmeter, both with a resolution of 0.1 μrad, were installed. The station is complemented with two pressure transducers, to control pore pressure, and four thermistors installed at different depths. Precipitation data is from Frankenforst manor, about 2 km away.
The data shows clear correlation between tilt, pressure and precipitation, as well as daily temperature-induced tilt oscillations. To decompose the tilt signal, we first differentiated the series three times with respect to time to separate the trend. We then expanded the remaining signal into a Fourier series that was truncated to cutoff signal corresponding to shorter periods than 10 days. This way we separate the seasonal variation from the shorter period residual component. The trend is predominantly linear, amounting to a 1000 μrad down slope tilt per year. The residual is characterized by rainfall events. We attempt to describe the tilt response to rain by a linear system, with precipitation data as input and tilt signal as output. The analysis shows that this model qualitatively explains several features of the tilt signal, but there is also a dependence of the tilt signal on pore pressure and temperature. The study shows that a continuous, high resolution monitoring of slope deformation allows decomposition into different processes and is thus a reasonable basis to verify theoretical models.

1. Introduction

The movement of landslides is a complex process that depends on many factors. No comprehensive theory exists, but several aspects have been well understood (e.g. Bromhead, 1992; Wilkinson et al., 2002). Some attempts have been made for a numerical simulation of landslide behavior, including kinematic and dynamic models (Angeli et al., 1999; Yalcinkaya and Bayrak, 2003) as well as hydrogeological aspects (Angeli et al., 1998, 2000; Brooks et al., 2004). The final aim is to obtain a better understanding of the underlying physics that might possibly allow to develop early warning systems (Bryant, 1991; Lollino et al., 2002).

The monitoring of landslide movement is normally based on inclinometers (Green, 1974; Moss et al., 1999; Konak et al., 2004). These instruments measure the tilt of the ground with a resolution of 0.1 mm/m and are read at intervals of weeks or months. For example, Stevens and Zehrbach (2000) interpreted 15 inclinometer readings taken through a time span of 6 years. The aim is to determine the existence and depth of shear horizons and the velocity of the shear movement. However, the low temporal resolution makes it difficult to understand details of the soil deformation processes, e.g. short-term relationship between external parameters, such as rainfall, temperature and groundwater table, and the movement of the sliding mass. We hypothesize that movement measurements at high resolution and high accuracy are required to provide data which may be used to verify theories and models (e.g. Xie et al., 2004) of soil deformation processes in landslide masses.

High resolution tiltmeters provide the same type of data as inclinometers, but at significantly higher resolution, i.e. between 1 μrad (≈1 μm/m) and 1 nrad (≈1 nm/m), depending on the tiltmeter model. Tiltmeters measure the angle between the instrument body and the plumb line in two horizontally perpendicular directions. Frequently used sensors in tiltmeters are spirit levels, within which the position of a gas bubble in an electrolytic fluid is sensed electronically, or small pendulums, where the position of a pendulum is sensed by a differential capacitor (Agnew, 1986). To achieve the high resolution in practice, tiltmeters require a very good coupling to the ground, i.e. they have to be installed at a fixed position like in boreholes or particularly prepared hollows. They cannot be moved during operation. Unlike inclinometers, tiltmeters measure only at one place and in one depth per instrument. A data logger automatically records the output of a tiltmeter at sampling periods, which can

* Corresponding author.
E-mail address: alejandro.garcia@pet.hw.ac.uk (A. García).
[1] Previous address: Geological Institute, Department of Applied Geophysics, Bonn University, Nussallee 8, 53115 Bonn, Germany.

0169-555X/$ – see front matter © 2009 Published by Elsevier B.V.
doi:10.1016/j.geomorph.2009.09.011

be freely adjusted by the user between second-fractions, minutes or days, and generates quasi-continuous high resolution data over long times of month and year. Thus, for landslide monitoring, tiltmeters might ideally supplement inclinometers, which are useful for measurements over a large depth-range in spatially distributed casings/boreholes, but with a comparatively poor resolution of amplitude and time. Mentes (2004) uses a typical setup with borehole tiltmeters of type Applied Geomechanics. Inc. 722A with 0.1 μrad resolution and shows tilt data from a landslide in Hungary.

This study aims at assessing the feasibility of high resolution tiltmeters for landslide monitoring. At the Dollendorfer Hardt landslide, we installed a monitoring station consisting of a borehole and a platform tiltmeter, three pressure transducers monitoring the groundwater table, and several thermistors. Rainfall data is available from a nearby Frankenforst research manor. We decompose the tilt data into movements at different time scales and show that there is a long-term tilt that is approximately linear with time. Finally, we analyze particular rainfall events. We apply linear system theory to determine transfer functions between rainfall and tilt response in order to compare events at different groundwater levels.

2. The field site and the experimental setup

The landslide under investigation is denoted "si7" and is located at the south facing side of the Dollendorfer Hardt hill-range near Bonn (Fig. 1). The slide has been investigated previously by other researchers (Schmidt and Dikau, 2005; Schmidt, 2001; Hardenbicker, 2004). Drillings indicate mainly two types of slide debris; an upper layer dominated by trachytic and basaltic fragments, and a lower layer composed predominantly of tertiary clays. The morphology of the slide is characterized by an upper scar zone with head scarp and four rotational blocks with visible minor scarps, a comparatively narrow transport zone (approx. 15 m wide and 4 m depth, as indicated by direct current electric resistivity profiles), distinguished by levees and remnant debris blocks, and the accumulation zone with toe failure and several tongues. The landslide is currently not being monitored other than by our station. Two major failure events have been identified and dated to 1958 and 1972 (Hardenbecker, 2004). Recent inclinometer investigations have displayed a moderate activity with displacements up to several cm/m per year (Schmidt and Dikau, 2005). Our monitoring station is situated in a remnant landslide block at the central transport zone, where the main down slope component runs in the north–south direction, with a small west–east component. A road was cut through the landslide mass a few m below the station (Fig. 2).

Fig. 3 gives an overview of the measurement setup. A borehole tiltmeter type AGI 722a Applied Geomechanics (Applied Geomechanics Inc, 1991) is installed in a borehole at nearly 3 m depth. The tiltmeter is vertically installed in compacted sand inside a PVC casing, cemented to the borehole walls in order to ensure an optimal coupling with the ground (see Fabian, 2004 for details). The platform tiltmeter, type AGI 701-2 Applied Geomechanics (Applied Geomechanics Inc, 1997), rests on a concrete platform lying above a tempered sand layer in a 30 cm

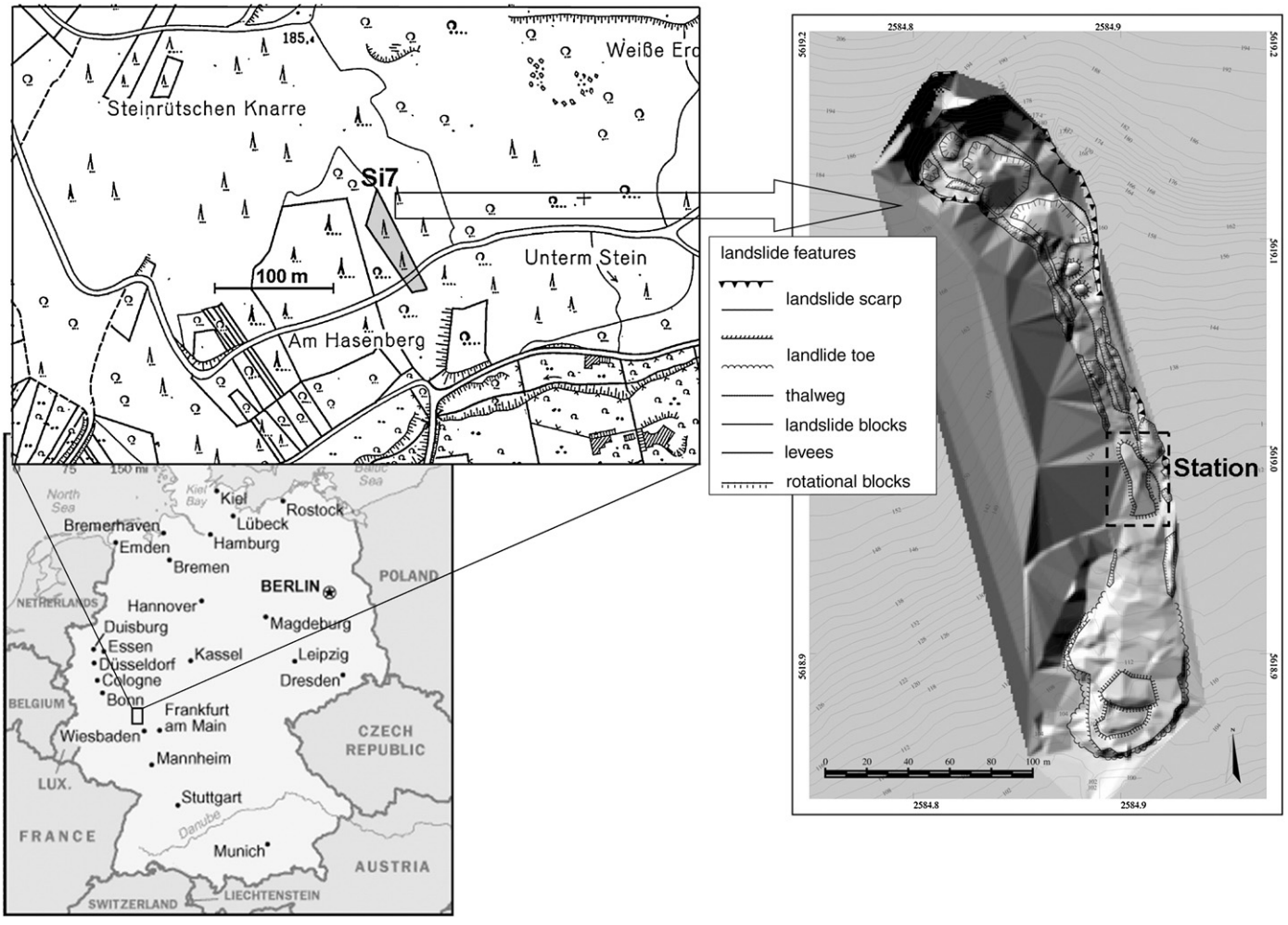

Fig. 1. Location of the "si7" landslide in Germany, with enlarged view of the Dollendorfer Hardt hill-range (top left panel), with the location of our experimental setup in grey. The right panel shows the sliding mass with the corresponding geomorphologic characteristics (after Schmidt and Dikau, 2005). The $+y$-axes for both tiltmeters point north and the $+x$-axes east.

Fig. 2. Photograph of the section of the landslide that includes the monitoring station. The boxes on the ground between the trees, contain the platform and the borehole tiltmeter (black arrow). The track cuts through the landslide.

deep hole, protected by a heavy iron casing. Both instrument types contain two independent electrolytic bubble tilt sensors (one for each tilt axis), of 0.1 μrad (1 μrad = 1 μm/m) nominal resolution, referred to as *x*- and *y*-direction. The measuring range is 8000 μrad. By convention, the *y*-axis is north-aligned, and thus the main down slope component is in negative *y*-direction. The tiltmeters are equipped with thermistors to control the instrument's temperature. Ground water level and soil pore pressure is controlled using two pressure transducers (Fabian, 2004): type In-Situ Inc. PXD-260 and PXD-261 (In-Situ Inc, 1989). Data is stored simultaneously for all the instruments and sensors, every 5 min by a 16 bit Squirrel type data logger (Grant instruments, 2003).

Note that the presumed shear plane is between 3 and 4 m (Schmidt, 2001). This is below the depth of the borehole tiltmeter; we are thus recording movements and deformations of a remnant landslide block within the sliding mass rather than the movement of the sliding mass as a whole.

3. Raw data

In the following, we first provide a brief overview of the data and describe some important features, before we proceed with the detailed analysis and the data decomposition. The data acquisition at the Dollendorfer Hardt began in mid December 2002 at a sampling rate of 1 min. Due to several gaps in the 2003 data, the discussion of the long-term behavior will be limited to the 2004 data set.

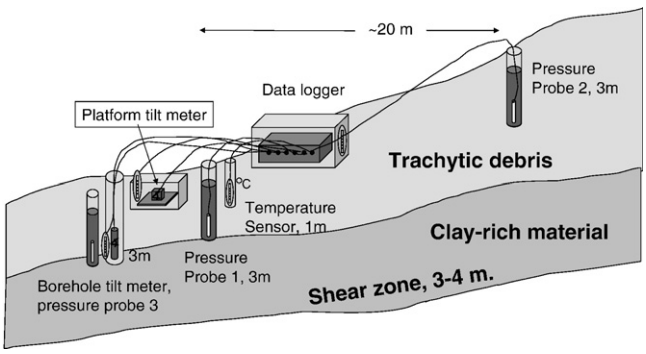

Fig. 3. Sketch of the station setup. The main instruments are the borehole tiltmeter and the platform tiltmeter, at a horizontal distance of approx. 3 m. Groundwater level is measured by pressure transducers in separate boreholes, one 1.5 m besides the tilt borehole, the second one about 20 m northwards uphill. The tiltmeters and the data logger are equipped with temperature sensors, and a separate thermistor was installed at 1.3 m depth.

3.1. Long-term behavior

Fig. 4 shows the borehole tilt data for the year 2004. The overall variation in the *x*-direction (perpendicular to slope) is significantly larger than the variation in the *y*-component (approx. 2000 μrad vs. 1000 μrad). The temporal development, although containing higher frequency variation, is clearly dominated by long-term variation down to a scale of 50 days. In particular the *x*-component seems to be composed of an annual variation overlain by a linear trend. A dominance of seasonal variation has been observed previously for a much longer time span (e.g. Kümpel et al., 2001 and references therein). The annual variation is correlated with the temperature, shown in Fig. 4 at 1 m depth. The tilt is delayed by approx. 50 days. This kind of information is essential to understand the thermoelastic response and to verify corresponding simulation codes.

3.2. Rain-induced deformation

Some of the short-term events (less than 10 days) in Fig. 4 are caused by rainfall. Prominent examples will be analyzed in the following section. The precipitation data is available from nearby Frankenforst manor, a research outpost operated by the University of Bonn, approx. 2 km away. For the *x*-component, regardless of the total average movement, one or two days after heavy rain (e.g. days 119 and 120), there is always a down slope (positive *x*) tilting of the top of the tiltmeter. Every such tilt change is followed by a slow decay back to the original state (compare Fig. 5: *x*-tilt first increases, then decreases back). The *y*-component behaves in the same way, where the tilt change is in the negative *y*-direction (also down slope, Fig. 5). In

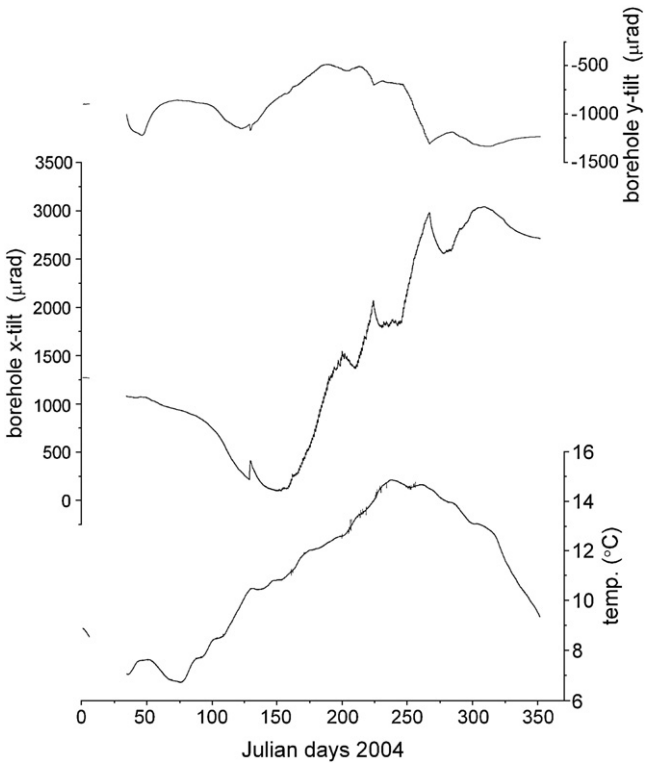

Fig. 4. Subsurface temperature at 1 m depth and borehole tilt measurements from the Dollendorfer Hardt for 2004. The time axis is given in Julian days, i.e. "0" corresponds to January 1. The *x*-component of the tilt signal is positive east, with a small down slope component, the *y*-component is positive north. The missing data before day 34 is due to limitations of the measuring range.

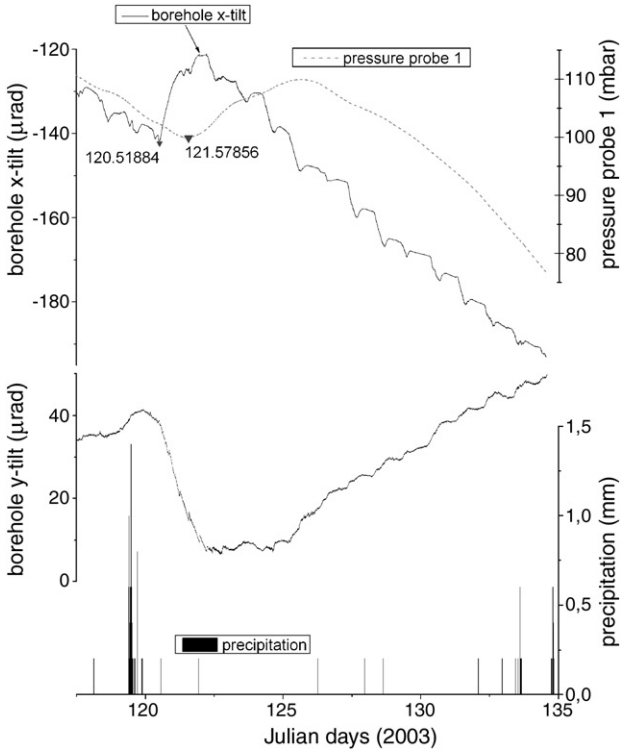

Fig. 5. Pore water pressure, precipitation and borehole tilt for a time span of 17 days around a selected rain event in 2003. Pressure probe 1 is located in close vicinity to the tiltmeter borehole. A variation of 1 mbar corresponds to a 1 cm change in well head.

the particular example shown in Fig. 5, the tilt signal starts changing approximately one day after the rain event and returns to the initial average movement some 10 days later. The rise of the groundwater table after the rainfall event is delayed with respect to the tilt by about one day. This implies that a direct mass loading effect is one cause of the tilt change.

An alternative way to represent the data is a hodograph (Fig. 6), where the *x*-tilt is plotted against the *y*-tilt. For the same rain event shown in Fig. 5 (days 119 and 120), down slope tilting is observed, larger for the main down slope component ($-y$), followed by the respective relaxation to the mean movement direction before rain falls.

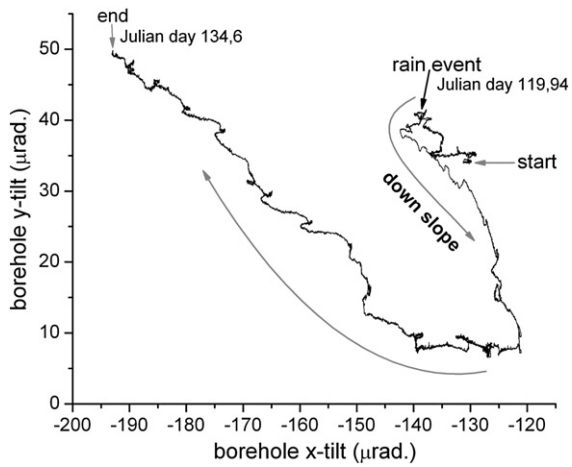

Fig. 6. Hodograph of the same rain event shown in Fig. 5, showing down slope tilting after the rain event. Small clockwise loops are caused by daily movements.

Diurnal variations are visible both in Figs. 5 and 6. These have been observed and discussed by other authors (Kümpel et al., 2001; Wosnitza, 1997; Fabian and Kümpel, 2003), and were attributed either to lateral changes in thermoelastic deformation or to subsurface pore pressure variation related to vegetation uptake. We confirm the observation that the phenomenon can vanish at certain periods, in our case preferably when the water table was low.

A topic of the study was the evaluation of the feasibility of the platform tiltmeter for this type of monitoring. Fig. 7 compares platform and borehole *x*-tilt data for another selected rainfall event in 2003 for a time span of 1 day. Although the high-frequency noise is stronger in the platform tiltmeter data, the data are obviously coherent with the data from the borehole tiltmeter, and thus useful down to a time scale of hours. This observation and similar data not shown here lead us to conclude that at this particular site, meteorological influence is not significantly larger on the surface platform tiltmeter than on the borehole instrument and does not inhibit its use for landslide monitoring. If this implication can be verified at other landslides as well, platform tiltmeters might become a useful alternative, because their installation is much simpler than the installation of the borehole tiltmeter, which requires a borehole 3–4 m deep of 30 cm diameter. As there is no coherent signal on a time scale below approx. 1 h, we increased the sampling interval at the end of March 2004 from 1 min to 5 min, in order to increase the maintenance interval of the station.

4. Data decomposition

Careful observation of the borehole tilt signals (Fig. 4) suggests the existence of several deformation components; a net movement or trend, a seasonal (possibly annual) movement and the residual, composed of high-frequency (periods less than a few days) fluctuations and isolated events. Assuming we have such a signal, given an

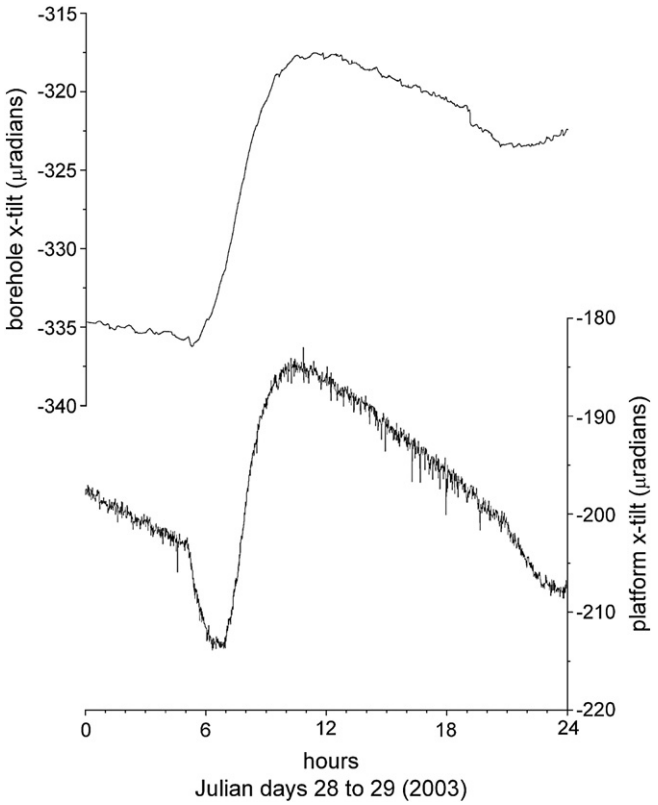

Fig. 7. *X*-component of tilt measured with the borehole tiltmeter (top) and the platform tiltmeter (bottom) for a selected rainfall event in 2003.

observable X_t (the measured tilt), we may consider a general model of the form,

$$X_t = \mu_t + S_t + Y_t \tag{1}$$

where μ_t denotes the time dependent mean of X_t (i.e. the trend), S_t is the seasonal component and Y_t is the residual, containing the rain effects, among other unidentified or unquantifiable variations.

4.1. The seasonal and trend behavior

In order to decompose the borehole tilt signals from 2004 into its different components, it was necessary to have a regularly sampled time series X_t, so the first step was to fill in the data gaps, by averaging adjacent points. Next, we resampled the data to a sampling rate of 1 h, again by averaging over adjacent data points. The purpose was to reduce computing effort in the subsequent processing. Since there was no coherent signal at periods shorter than 1 h, this step does not affect the result. Further, inspection of the original data had shown that the direct effect of a rain event has decayed after 10 days. Thus, we defined all signal with periods shorter than 10 days as residual component Y_t, and signal with longer periods to be either due to the trend or the seasonal component.

The decomposition scheme is schematically illustrated in Fig. 8. The strategy is to eliminate the trend by differentiation, and to remove the residual by expanding the signal into a Fourier series that is truncated after the term corresponding to the appropriate frequency. Because differentiation increases high-frequency noise, it turned out useful to reduce the residual first by averaging the data over 10 days.

For the long-term trend μ_t, a linear function seems a plausible assumption. However, we did not want to impose this as a restriction, because a continuous acceleration might be present in the data. Therefore, we assumed a second order polynomial for the long-term behavior. Thus, in order to separate the trend from the signal, we differentiated the low-pass filtered signal three times with respect to time:

$$\frac{\partial^3}{\partial t^3} X_t = S_t''' + Y_t''' \tag{2}$$

where the $'''$ denotes triple differentiation for convenience. The differentiated signal X_t''', was then expanded in a Fourier series, including terms up to $n = 35$. With the total length of the time series T being roughly 350 days, $n = 35$ corresponds to a truncation period of 10 days, and the truncated Fourier expansion reads:

$$S_t''' = \sum_{n=1}^{35} x(\omega_n) e^{i\omega_n t} \tag{3}$$

where $\omega = 2\pi n/T$. Subsequently, the differentiated seasonal term S_t''' was integrated three times to reconstruct the seasonal component, without any high-frequency contributions nor any time-trend, i.e. all components with up to second order time-dependence have been removed. The result is a band pass filtered signal that contains neither a trend nor high-frequency components (Fig. 9), which we call seasonal component.

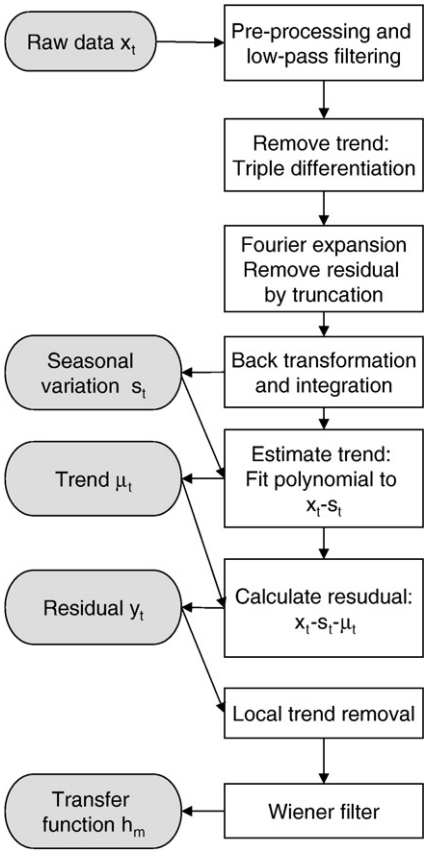

Fig. 8. Block diagram of decomposition scheme. The left column denotes input and output data, the right column describes the different processing steps.

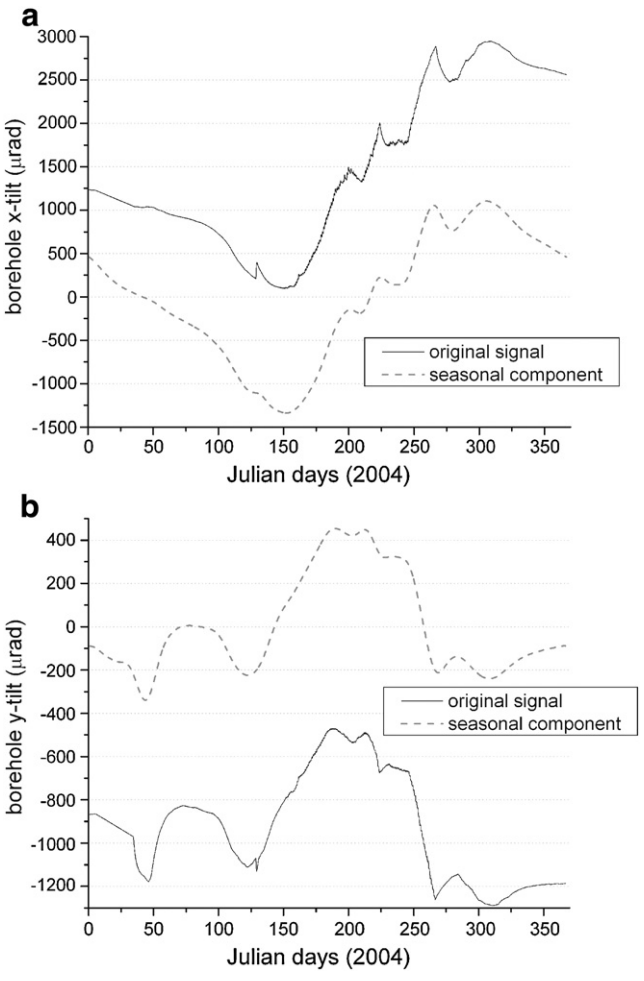

Fig. 9. Original signal, X_t (solid line), and seasonal component S_t (dotted line) for x-component (panel a) and y-component (panel b) of the borehole tilt.

Having determined the seasonal component, we can now subtract it from the original signal to obtain the trend, with the residual superimposed:

$$Y_t + \mu_t = X_t - S_t. \quad (4)$$

We then use a least-squares method to fit a second order polynomial to the curve and obtain the trend (Fig. 10). The best fit by the least-squares method, for the *x*- and *y*-tilt reads:

$$\mu_t = 902.6 + 3.658t - 0.001t^2$$
$$\mu_t = -763.896 - 0.885t - 7.61 \times 10^{-5}t^2. \quad (5)$$

Here, t is given in days and μ_t in microradians (for both tilt components). Obviously, the coefficients of the first order terms are much larger than those of the second order terms, and omitting the second order term would not significantly change the result. Therefore, we conclude that the dominating long-term trend is linear without any acceleration or deceleration. The linear coefficients in Eq. (5), positive for the *x*- and negative for the *y*-coordinate, indicate the direction of the net movement, i.e. down slope tilt in both cases.

Fig. 11 shows the original data and the signal composed of trend and seasonal variation. Apparently, these two dominate the measured signal, which is why the mismatch between calculated and measured curve is small. We obtain the residual by subtracting the trend and seasonal variation from the measured signal:

$$Y_t = X_t - \mu_t - S_t. \quad (6)$$

The resulting residual curves are shown in Fig. 12. They are composed of rain-induced deformation and other variations.

In the following, we will have a closer look at the rain-induced deformation. Westerhaus and Welle (2002) described rainfall effects as a combination of loading and a pore pressure effect and successfully explained tilt signals at Merapi volcano (Indonesia). Here, we adopt a more general approach and try to establish a relationship between rainfall data and tilt without assuming a physical model. One important aspect is whether the relationship between rainfall and deformation may be described by a linear system, where the rainfall is the input and the tilt signal is the output. In that case it should be possible to find one impulse response or transfer function which allows to predict the induced tilt signal from the rainfall data for all rainfall events. This would have important implications for the description and simulation of the landslide movement, and the impulse response itself might be used to determine properties of the sliding mass. The transfer functions are also useful to compare different rainfall events, because they are independent of the particular rainfall function.

In order to evaluate whether a linear system is a useful description, we first determine a transfer function for a particular rain event. We then apply the same transfer function to other rain events and see how well we can predict to evaluate the quality of the deformation

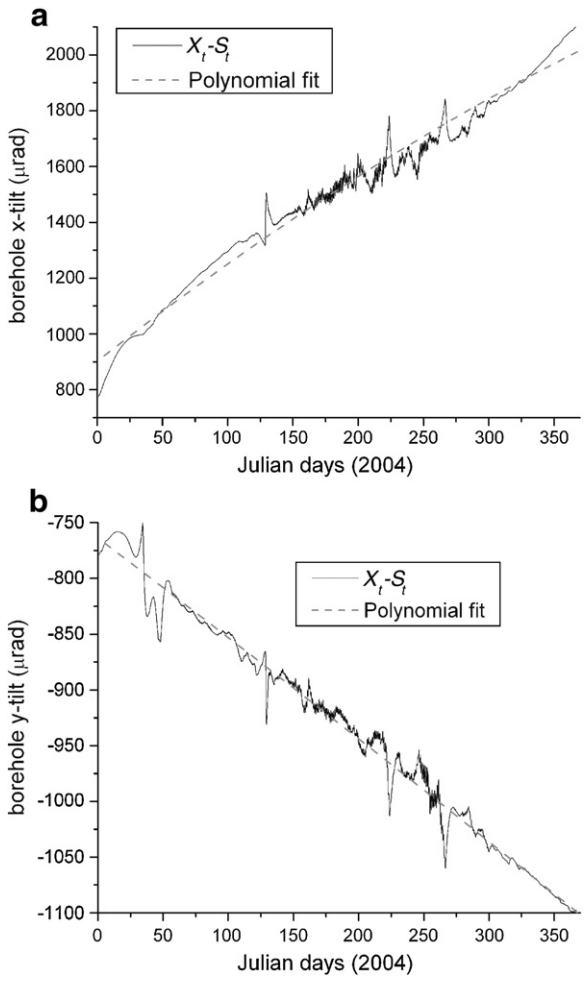

Fig. 10. Tilt signal with seasonal movements removed (X_t–S_t, solid line), with least-squares fit representing the trend component (μ_t, solid line). Both *x*-tilt (panel a) and *y*-tilt (panel b) are shown.

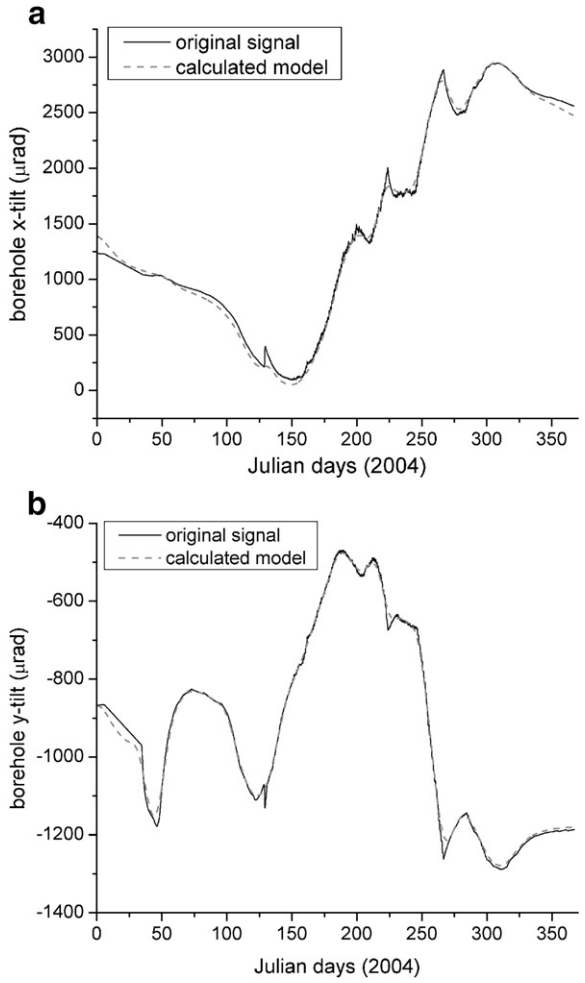

Fig. 11. Original tilt data (X_t, dotted line) and signal composed of trend and seasonal variation ($\mu_t + S_t$, solid line) for *x*- and *y*-component of the borehole instrument.

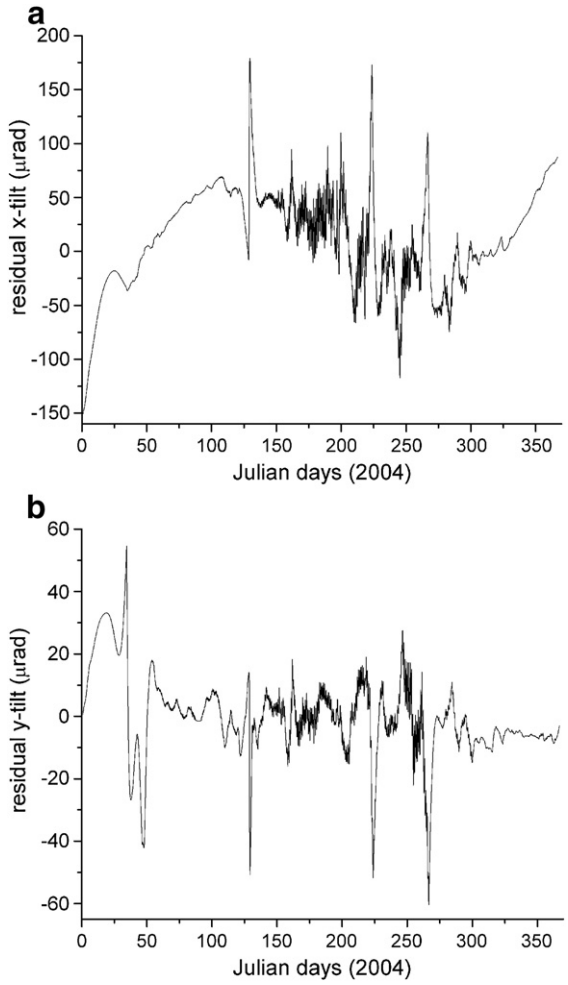

Fig. 12. Calculated residual, Y_t, obtained after subtracting the seasonal and trend components from the original data, for both the borehole *x*- (Fig. 10a) and *y*-tilt (Fig. 10b) components.

prediction. Assuming a linear system implies that the tilt signal may be described as a convolution of rainfall data and the transfer function:

$$y_1 = \sum_{m=0}^{M} h_m z_{j-m},\ j = 0, 1, 2, \ldots, \tag{7}$$

or more compactly

$$y_j = h_j * z_j, \tag{8}$$

where h_j is the transfer function to be determined, z_j is the input data set (the rainfall data) and the * symbol denotes convolution. The number of points of the transfer function M was chosen such that a sufficient number of degrees of freedom were obtained. The transfer function is determined by minimizing the root mean square (RMS) difference between the measured tilt data, denoted d_j, and the calculated output using Eq. (7) (Buttkus, 1991):

$$\frac{\partial}{\partial h_1} \sum_{j=1}^{M} \left(h_j * z_j - d_j\right)^2 = 0,\ l = 0, \ldots, M. \tag{9}$$

The process to determine the h_j has been described by Wiener (1949), and leads to the application of a linear filter called optimum filter or Wiener filter.

To obtain a transfer function h_m, we have to isolate rain-induced tilt. In a first step, we select rain events where the rainfall is impulse-like, because it is numerically more stable to find transfer functions in that case. To separate these rain events from the general background movement, we subtract a local trend for each rainfall event, as illustrated in Fig. 13. It is apparent from Figs. 10 and 12 that simply subtracting the general trend and the seasonal variation from the signal is not sufficient, because there is residual variation that is not associated with rainfall.

We calculated the transfer functions as optimal filters for several rain events, those produced by more or less isolated rain activities, so that the rain-induced movements could be separated from the "background movement". In Fig. 14, we show the measured tilt signal (d_j in Eq. (9)) and the calculated signal y_j as given by Eq. (7) for four examples. All RMS errors are low, and the curves match very well in general. This means that it is generally possible to find a linear transfer function for each separate rain event. Even in the case where the rainfall is spread over a longer time span (Fig. 14b) the shape of the tilt signal can be reproduced fairly well.

The four examples are labeled according to the average groundwater level over the time span of the measured signal, where "high" corresponds to <2 m below surface, "intermediate" to 2–3 m below surface and "low" to >3 m.

The next step is to examine whether the calculated transfer functions are independent of the actual conditions at the time of the particular rain event. For this purpose, we convolved the transfer functions determined for one event with the precipitation data from another event to assess whether the measured tilt signal may be predicted this way. The top left panel of Fig. 15 shows the measured tilt response to an isolated rainfall event at a high groundwater level together with a predicted tilt response that was calculated by convolving the rainfall data from this event with a transfer function determined from another event, also at high groundwater level. The amplitude of the signal is well matched, but there are differences in shape, manifested by a steeper increase of the measured signal compared to the predicted one. The top right and bottom left panels compare predicted and measured signals where the groundwater levels are intermediate and high, respectively. In both cases, the signal corresponding to a high groundwater level decays back to the original state about one day earlier. In the bottom right panel, the predicted signal is determined from a low groundwater transfer function and compared with the high-level measured signal. Here, the predicted signal has a shorter decay time (total duration about 2 days vs. 3 days) and smaller amplitude than the measured one. The fact that decay times are smallest at low groundwater level, and largest at intermediate levels indicates that there is no simple relationship between decay time and groundwater level. We may conclude that both the direct mass loading effect and the water penetrating into the ground, increasing the pore water pressure, are important processes that interact with each other (and with further processes not considered here) in a nonlinear fashion. As a result, including the pore water pressure data from the pressure probes directly to predict a theoretical tilt signal in a causal system as described by Eq. (7) is not feasible, because the measured tilt signal precedes the rise of the groundwater table.

In summary, the description of the relationship between rainfall and deformation as a linear system is able to reproduce certain features, but nonlinear effects are significant and there is a clear dependence on the pore water pressure conditions.

5. Discussion

With the monitoring setup used at the Dollendorfer Hardt landslide, we obtain ground-dynamics information on internal movement within the landslide body. The borehole instrument at 3 m depth is above the shear zone (at 4 m), and thus we do not directly see the

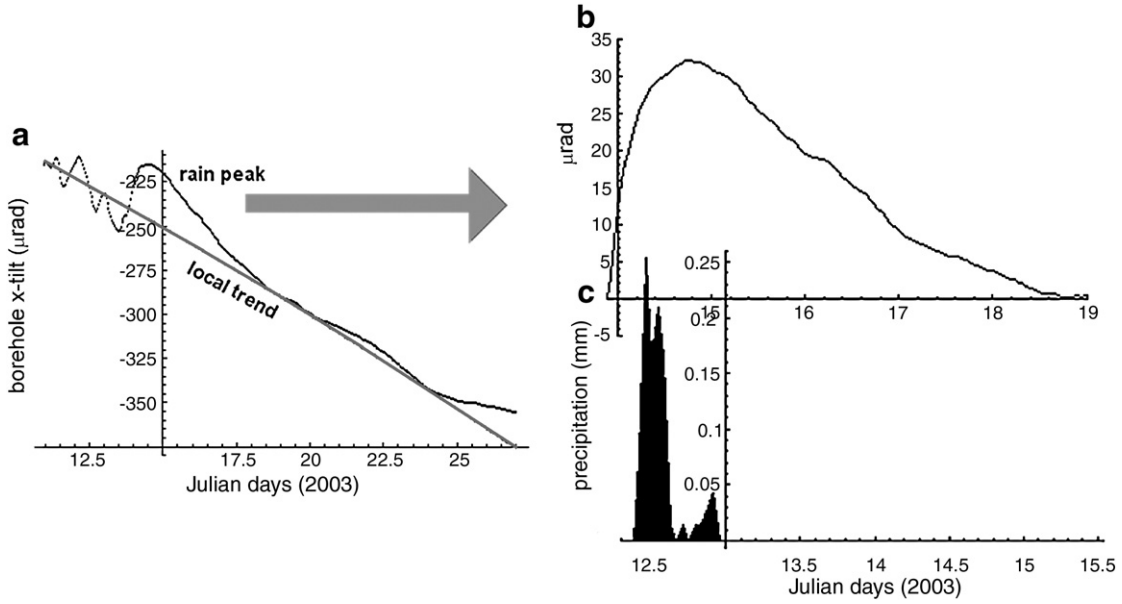

Fig. 13. Panel a: Original tilt data from January 2003. We identified rain-induced tilt with its respective precipitation precursors (b) and removed the local trend from the signal, to obtain the desired impulse response (c).

shearing process. However, the internal deformation and the overall movement are closely related to the shearing, and thus our data are an important indicator of the landslide activity. Tilt meter measurements provide highly accurate information at a high resolution in time, allowing for a decomposition of the deformation and a detailed analysis of the relationship with pore water pressure, temperature and rainfall at different time scales. Thus, they may establish as an important supplement to standard inclinometer measurements, which have a lower accuracy and lower resolution in time, but are less expensive than tilt meters. Inclinometers are usually installed along a vertical profile, with the main purpose to monitor the movements along the shear zone. A combination of the two types of measurements could enable a comprehensive understanding of the deformation processes within a sliding mass.

The decomposition scheme we suggest requires several decisions to be made or parameters to be chosen. First, when isolating the long-term behavior, we chose a second order polynomial. We concluded that the dominating long-term trend is linear, and a closer look at Eq. (5) shows that the maximum value of the second order term is

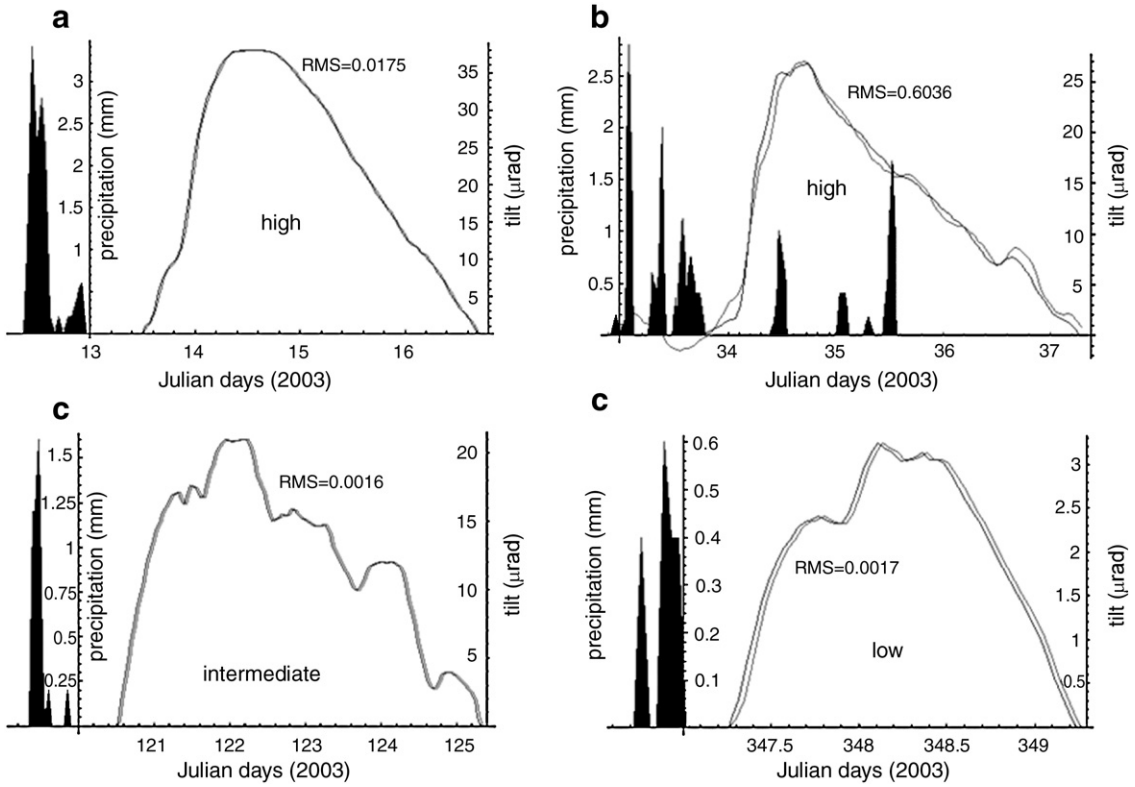

Fig. 14. Tilt data for 4 different isolated rain events (solid lines) and calculated signals (dotted lines) obtained by convolving the transfer functions with the corresponding rainfall data. The labels "high", "intermediate" and low indicate the average groundwater level. Root mean square errors are given in microradians.

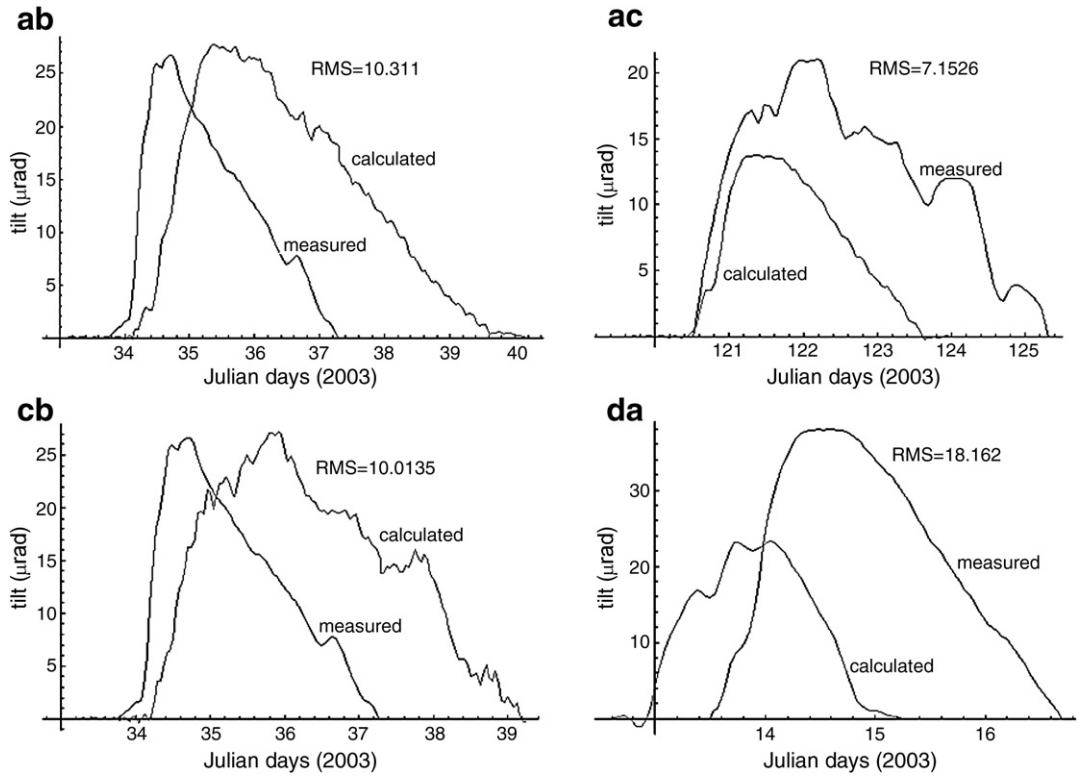

Fig. 15. Measured tilt signals and predicted data obtained by convolving the transfer function with the appropriate rainfall input. Figures are labeled according to the event used to determine the transfer function and the rainfall data, i.e. (ab) means transfer function determined from event (a) (Fig. 14) convolved with rainfall data from event (b). Solid lines correspond to original signals and dotted curves to the predicted ones.

133 μrad within one year, which is well below the maximum amplitude of the seasonal variation. Thus, using a linear long-term trend would slightly alter the seasonal variation, but not enough to affect any of the conclusions. The second decision refers to the threshold period to distinguish between seasonal variation and residual signal, which was set to 10 days based on visual inspection of the data after rainfall events. This definition is subjective, but useful for our purposes because it simplifies the analysis of rainfall as an isolated process. The choice of the threshold is not critical, because the main difficulty lies in the separation of the tilt response to rainfall from other residual deformation processes. Future work might involve a coherency analysis of the full time series, without assumptions on the length of a rainfall response.

We have identified three different components in our tilt signal: A long-term linear trend, a seasonal variation, and the residual signal consisting of rain-induced deformation and other processes. The residual signal with maximum amplitudes of about 100 μrad has periods less than 10 days and contributes smallest to the overall variation. One important observation after rainfall induced tilt is the decay of the signal back to the initial state. This implies that the general state of the system is stable and not sensitive to small distortions. Our attempt to describe the rain effect as a linear system, with precipitation data as input and tilt signal as output, is able to reproduce certain features qualitatively. However, we also have seen that there are significant nonlinear effects. This means that it is not possible to find a single transfer function that quantitatively describes the system independent of the current state of the landslide. This is no surprise, because a dependence of the tilt response to rainfall on pore pressure and temperature might be expected. Westerhaus and Welle (2002), successfully explained the tilt response to rainfall by a combination of loading effect and infiltration effect. However, their data are from Merapi volcano and were not measured on a landslide. The lithology is different in that there is no clay below the volcanic sediments. Thus, although they do not show groundwater level data, it can be assumed that in our case we have more saturated conditions, and thus our results are complimentary.

The seasonal variation (periods greater than 10 days) has maximum amplitudes of approx. 2000 μrad, about one order of magnitude larger than the residual variation. The amplitude of the *x*-component, which is almost perpendicular to the slope, is larger than that of the down slope *y*-component (2000 vs. 800 μrad), indicating a complex deformation pattern. The correlation with temperature and the characteristic period of one year imply that thermoelastic deformation is one important factor. The phase shift of about 50 days between tilt signal and temperature can be attributed to the diffusive properties of thermal conduction. Schmidt and Dikau (2005) also identified seasonal variation from their inclinometer measurements and refer to Yamada (1999), who explained similar observations with swelling/shrinking cycles of saturated soils. Our results seem to be consistent with their findings and support the hypothesis of an elastic behavior.

The most important finding may be the existence of the long-term trend, with amplitudes of approximately 1000 μrad/year (= 1 mm/m/year). Schmidt and Dikau (2005) mention the possibility of an increasing failure probability due to the continuous destabilization caused by the moving material of the transport zone. Our results are consistent with their conclusions and provide further evidence for a continuous movement separated from the elastic seasonal variation.

6. Conclusions

We used high resolution tiltmeters to measure the internal deformation inside a landslide body. The highly accurate data and the dense sampling permit the decomposition of the movement into different components. The tilt signal is dominated by long-term variation on a time scale of weeks to months. The long-term variation may be further decomposed into a trend that was shown to be predominantly linear, and a seasonal variation. The trend and the seasonal variation are approximately the same order of magnitude in

amplitude (roughly 1000 μrad/year=1 mm/m/year). The trend indicates that the landslide undergoes small but continuous deformation. The short-term variation (periods less than 10 days) is dominantly rain-induced. After a rain event, the signal decays back to its initial value. The response depends on the state (mainly the groundwater level) of the landslide system, and therefore some features cannot be described with a single linear transfer function.

A platform tiltmeter, even though it is more exposed to surface noise, i.e. vibrations caused by wind on the nearby trees, direct impact by rain, animal activity, etc., provided useful and accurate data. In our particular application, the noise is only a few μrad larger than for the borehole, which is perfectly acceptable for the purpose of landslide monitoring. The simple installation and maintenance makes these tiltmeters a viable addition to the more cumbersome borehole instruments.

Future work should attempt to combine inclinometer measurements and high resolution tilt measurements with numerical simulation, using the data to verify the modeling results. The separation of the signal into its different components should facilitate the modeling and the verification, because it might not be necessary to take into account all phenomena at the same time. The final aim is to identify the important physical processes, which will then be a useful basis for a later development and modification of risk management strategies for landslides.

Acknowledgements

The original installation of the tiltmeters was supported by the Deutsche Forschungsgemeinschaft (SFB 350) and by Prof. Kümpel. Uwe Börst kindly provided the precipitation data. The comments of Jochen Schmidt, who kindly provided the original of a panel of Fig. 1, and two anonymous reviewers considerably improved the manuscript. We thank Thomas Glade for encouraging us to submit the manuscript to this special issue.

References

Agnew, D.C., 1986. Strainmeters and tiltmeters. Review of Geophysics 24 (3), 579–624.
Angeli, M.-G., Buma, J., Gasparetto, P., Pasuto, A., 1998. A combined hillslope hydrology/stability model for low-gradient clay slopes in the Italian dolomites. Engineering Geology 49, 1–13.
Angeli, M.-G., Pasuto, A., Silvano, S., 1999. Towards the definition of slope instability behaviour in the Alverà mudslide (Corina d'ampezzo, Italy). Geomorphology 20201–211.
Angeli, M.-G., Pasuto, A., Silvano, S., 2000. A critical review of landslide monitoring experiences. Engineering Geology 55, 133–147.
Applied Geomechanics Inc, 1991. User's Manual: 722 Borehole Tiltmeter. Santa Cruz, USA.
Applied Geomechanics Inc, 1997. User's Manual: 700-Series Platform and Surface Mount Tiltmeters. Santa Cruz, USA.
Bromhead, E.N., 1992. The Stability of Slopes. Second Edition. Blackie Academic & Professional, London.
Brooks, S.M., Crozier, M.J., Glade, T.W., Anderson, M.G., 2004. Towards establishing climate thresholds for slope instability: use of physically-based combined soil hydrology–slope stability-model. Pure and Applied Geophysics 161, 881–905.
Bryant, E., 1991. Natural Hazards. Cambridge University Press.
Buttkus, B., 1991. Spektralenanalyse und Filtertheorie in der angewandte Geophysik. Springer-Verlag.
Fabian, M., 2004. Near surface tilt and pore pressure changes induced by pumping in multi-layered poroelastic half-spaces. Bonn University, Dissertation.
Fabian, M., Kümpel, J.-M., 2003. Poroelasticity: observations of anomalous near surface tilt induced by ground water pumping. Journal of Hydrology 281, 191–209.
Grant Instruments, 2003. Manual: Squirrel SQ1600 Data Logger. Grant Instruments (Cambridge) Ltd, Shepreth Cambridgeshire SG8 6GB. http://www.grant.co.uk/.
Green, G.E., 1974. Principles and performance of two inclinometers for measuring horizontal ground movements. Field instrumentation in geotechnical engineering, vol. 8, pp. 166–179.
Hardenbicker, U., 2004. Hangrutschungen im Bonner Raum - Naturräumliche Einordnung und ihre anthropogenen Ursachen. Arbeiten zur Rheinischen Landeskunde, 64.
In-Situ Inc, 1989. Submersible Pressure Transducer Model PXD-260, Operator's Manual. Laramie, USA.
Konak, G., Onur, A.H., Karakus, D., Köse, H., Koca, Y., Yenice, H., 2004. Slope stability analysis and slide monitoring by inclinometers readings: Part 2. Mining Technology 113, 171–180.
Kümpel, H.-J., Lehmann, K., Fabian, M., Mentes, G., 2001. Point stability at shallow depth — experience from tilt measurements in the lower Rhine embayment, Germany, and implications for high resolution GPS and gravity recordings. Geophysical Journal International. 146, 699–713.
Lollino, G., Arattano, M., Cuccureddu, M., 2002. The use of automatic inclinometric system for landslide early warning: the case of Cabella Ligure (North-Western Italy) Physics and Chemistry of the Earth, vol. 27, pp. 1545–1550.
Mentes, Gy., 2004. Landslide monitoring by borehole tiltmeters in Dunaföldvar. In: Mentes, Gy., and Eperne, I., (Eds.), Landslide monitoring of loess structures in Dunaföldvar, Hungary, 86 pp. Geodetic and Geophysical Research Institute, Hungarian Academy of Sciences, Sopron. ISBN: 9638381213, 67–76.
Moss, J.L., McGuire, W.J., Page, D., 1999. Ground deformation monitoring of a potential landslide at La Palma, Canary Islands. Journal of Volcanology and Geothermal Research 94, 251–265.
Schmidt, J., 2001. The role of mass movements for slope evolution, Dissertation, Bonn University.
Schmidt, J., Dikau, R., 2005. Preparatory and triggering factors for slope failure: analyses of two landslides near Bonn, Germany. Zeitschrift für Geomorphologie 49 (1), 121–138 Issue 1.
Stevens, W.R., Zehrbach, B.E, 2000. Inclinometer data analysis for remediated landslides. In: Marr, A. (Ed.), Geotechnical measurements; lab and field: Geotechnical Special Publication, 106, pp. 126–137.
Westerhaus, M., Welle, W., 2002. Environmental effects on tilt measurements at Merapi volcano. Bulletin d'informations marees terrestres (BIM). Proceedings of the Meeting on Environmental Effects on the Gravity Vector in Jena.
Wiener, N., 1949. Extrapolation, Interpretation and Smoothing of Stationary Time Series. John Weley and Sons, New York.
Wilkinson, P.L., Anderson, M.G., Lloyd, D.M., 2002. An integrated hydrological model for rain-induced landslide prediction. Earth Surface Processes and Landforms 27, 1285–1297.
Wosnitza, E.M., 1997. Schriftenreihe des SFB 350, No. 66, Diplom thesis, Univ. Bonn.
Xie, M., Esaki, T., Cai, M., 2004. A time-space based approach for mapping rainfall-induced shallow landslide hazard. Environmental Geology 46, 840–850.
Yalcinkaya, M., Bayrak, T., 2003. Dynamic model for monitoring landslides with emphasis on underground water in Trabzon Province, northeastern Turkey. Journals of Surveying Engineering. 129 (3), 115–124.
Yamada, S., 1999. The role of soil creep and slope failure in the landscape evolution of a head water basin: field measurements in a zero order basin of northern Japan. Geomorphology, 28, 329–344.